

ORIGINAL
RESEARCH

M. Hatakenaka
Y. Shioyama
K. Nakamura
H. Yabuuchi
Y. Matsuo
S. Sunami
T. Kamitani
T. Yoshiura
T. Nakashima
K. Nishikawa
H. Honda



Apparent Diffusion Coefficient Calculated with Relatively High b-Values Correlates with Local Failure of Head and Neck Squamous Cell Carcinoma Treated with Radiotherapy

BACKGROUND AND PURPOSE: Few studies have investigated the relationship between ADC and clinical outcome in HNSCC. Our hypothesis was that relatively high pretreatment ADC would correlate with local failure of HNSCC treated with radiation therapy.

MATERIALS AND METHODS: This includes prospective and validation studies. Seventeen patients treated with radiation therapy for primary HNSCC completed the prospective study. Variables considered to affect local failure including MR imaging-related parameters such as ADC and its change ratio were compared between patients with local failure and controls, and those showing difference or association with local failure were further tested by survival analysis. Furthermore, variables were analyzed in 40 patients enrolled in the validation study.

RESULTS: Relatively high ADC calculated with b-values (300, 500, 750, and 1000 s/mm²) before treatment, high ADC increase ratio, and treatment method (chemoradiotherapy versus radiation therapy alone) revealed significant difference between patients with local failure and controls or association with local failure. In Cox proportional hazard testing, high ADC before treatment alone showed significant association with local failure ($P = .0186$). In the validation study, tumor volume before treatment, high ADC before treatment, T stage (T12 versus T34), and treatment method showed significance. Tumor volume before treatment ($P = .0217$) and high ADC before treatment ($P = .0001$) revealed significant association with local failure in Cox proportional hazard testing. High ADC before treatment was superior to tumor volume before treatment regarding association with local failure.

CONCLUSIONS: These results suggest pretreatment ADC obtained at high b-values as well as tumor volume correlate with local failure of HNSCC treated with radiation therapy.

ABBREVIATIONS: ADC = apparent diffusion coefficient; AUC = area under the curve; DWI = diffusion-weighted imaging; GTV = gross tumor volume; HNSCC = head and neck squamous cell carcinoma; NPV = negative predictive value; PPV = positive predictive value; ROC = receiver operating characteristic; ROI = region of interest; SI = signal intensity.

The self-diffusion of cell water is affected by temperature and viscosity as well as by barrier structures such as cell membranes^{1,2}; thus, DWI reflects microstructural information about tissues. However, it is difficult to evaluate in vivo the relation between diffusive parameters and tissue microstructure without changing other factors, such as temperature and viscosity, which would affect proton diffusion. We have shown that changes in tissue microstructure directly affect the proton diffusion parameters.^{3,4} Based on the concept that the ADC reflects the tissue microstructure, the ADC has been used to differentiate malignant from benign conditions: malignancies have been reported to show lower ADC than benign lesions, owing to the high cellularity of the former.⁵⁻⁹

Received October 21, 2010; accepted after revision February 14, 2011.

From the Departments of Clinical Radiology (M.H., Y.S., Y.M., S.S., T.K., T.Y., H.H.), Health Sciences (H.Y.), and Otorhinolaryngology (T.N.), Graduate School of Medical Sciences, Kyushu University; Department of Radiology (K.Na.), Kyushu University Hospital at Beppu; and Radiology Center (K.Ni.), Kyushu University Hospital, Fukuoka City, Japan.

Please address correspondence to Masamitsu Hatakenaka, MD, PhD, Department of Clinical Radiology, Graduate School of Medical Sciences, Kyushu University, 3-1-1 Maidashi, Higashi-ku, Fukuoka City, 812-8582, Japan; e-mail: mhatake@radiol.med.kyushu-u.ac.jp

Indicates article with supplemental on-line tables.

<http://dx.doi.org/10.3174/ajnr.A2610>

Recent studies have successfully used ADC to predict treatment response, revealing that pretreatment ADC correlates with treatment response¹⁰⁻¹³ and that the changes in ADC at an early treatment phase also can predict treatment response.¹⁴⁻¹⁸ Although chemoradiotherapy is a good approach for the treatment of HNSCC because it minimizes functional and social losses arising from surgery such as eating and/or speech impairment and cosmetic problems, there have been few studies about the usefulness of ADC as a surrogate marker of treatment response of HNSCC.¹⁹⁻²³ Furthermore, the method of calculating ADC remains controversial, and it is also still not clear whether pretreatment ADC or ADC change at the early treatment phase is more practical for predicting treatment response.

We hypothesized that pretreatment ADC calculated with relatively high b-values would correlate with local failure of HNSCC treated with radiation therapy.

Materials and Methods

This study included a prospective pilot study to determine clinical and imaging variables related to local failure and a validation study to confirm the results of the prospective study; both were approved by the Committee on Clinical Study at our institution. Some patients

analyzed in the present study overlapped with those of our previous study²³; however, the variables and methods used for analysis are different.

Patients

Informed consent was obtained from each participant for the prospective study. We enrolled 32 patients who were histologically proved to have primary HNSCC in our institute between April 2006 and July 2008 and who were scheduled to receive radical radiation therapy (>60 Gy to GTV). Patients with a diagnosis of nasopharyngeal cancer were not enrolled because the characteristics of nasopharyngeal cancer are different from those of other types of HNSCC. Nasopharyngeal cancer is known to be more radiosensitive than other types of HNSCC.²⁴ Among the 32 patients enrolled, 3 were excluded because detection of the primary lesion on DWI was difficult due to small lesions or artifacts, 7 were excluded because early-phase MR imaging could not be obtained or the lesion could not be detected clearly on the early-phase imaging, and 5 were excluded because the radiation dose to the GTV was <60 Gy due to poor patient condition or severe side effects. Therefore, 17 patients (15 men; age range, 37–85 years; median age, 64 years; 7 oropharynx, 8 hypopharynx, 1 larynx, 1 oral cavity) who received radiation therapy with a radiation dose to GTV >60 Gy (range, 64–71 Gy, median, 65.4 Gy) and who had MR images both before treatment and at the early phase of treatment were studied. No patient had a history of receiving chemotherapy or radiation therapy.

For the validation study, 40 patients in total (37 men; age range, 37–85 years; median age, 64 years; 15 oropharynx, 19 hypopharynx, 4 larynx, 2 oral cavity) who had received radiation therapy with a radiation dose to GTV >60 Gy (range, 64–71 Gy; median, 65.4 Gy) between April 2006 and June 2009 and had pretreatment MR imaging including DWI were retrospectively studied. They included 17 patients in the prospective study, 5 of the 7 patients who were excluded from the prospective study because of the lack in MR imaging at an early phase of treatment or the difficulty of detecting lesions on early-phase MR imaging (the remaining 2 patients were not included because they showed local control but the follow-up period was <10 months), and an additional 18 patients who were not enrolled in the prospective study. Informed consent was waived for the retrospective study. No patient had a history of receiving chemotherapy or radiation therapy.

Treatment and Follow-Up

External radiation therapy was performed with 4- or 6-MV x-ray in 1.8–2.0-Gy fractions at 5 fractions per week by using a 3D conformal technique. In the prospective study, concurrent chemoradiotherapy (TS-1 [Tahio Pharmaceutical, Tokyo, Japan] dose of 65 mg/m² for 4 weeks followed by 2 weeks of rest while receiving radiation therapy) was given to 13 patients, and the remaining 4 patients were treated with radiation therapy alone due to their condition. TS-1 contains tegafur, gimeracil (5-chloro-2,4-dihydrogenase), and potassium oxonate at a molar ratio of 1:0.4:1. In the validation study, concurrent chemoradiotherapy was performed for 35 patients (TS-1 for 32 patients and cisplatin for 3 patients, 5 mg/m² for 5 days a week while receiving radiation therapy) and the remaining 5 patients were treated with radiation therapy alone due to their condition. The overall treatment time was defined as the number of days from the start of treatment to the end of treatment.

Patients were followed up for the evaluation of local control. The follow-up evaluation included physical, endoscopic, and radiologic

examinations. Contrast-enhanced CT was the base of the radiologic examination, and MR imaging and/or fluorodeoxyglucose–positron-emission tomography/CT were obtained when otorhinolaryngologists considered these examinations were necessary. Histologically confirmed local recurrences during follow-up were considered as local failure. The follow-up period was designated as the total time of follow-up starting at treatment initiation and ending either at histologically confirmed local failure or at last patient contact without local failure. As for the prospective study, 8 patients developed local failure and the remaining 9 patients showed local control during the follow-up period. The follow-up time of patients with local failure ranged from 2.1 to 15.8 months, with a median of 4.6 months. That of patients with local control ranged from 10.5 to 42.7 months, with a median of 23.6 months. All cases but 1 showed local recurrence within 8 months of follow-up; thus, we considered those showing no local recurrence after >10 months of follow-up as local control. As a salvage therapy for lymph node recurrence in patients with local control, transarterial infusion of cisplatin was performed in 1 case.

For the validation study, 13 patients developed local failure, and the remaining 27 showed local control during the follow-up period. The follow-up time of patients with local failure ranged from 2.1 to 17.5 months, with a median of 4.9 months. That of patients with local control ranged from 10.5 to 42.7 months, with a median of 16.4 months. As a salvage therapy for lymph node recurrence in patients with local control, lymph node dissection was performed in 3 cases and transarterial infusion of cisplatin was performed in 2 cases.

MR Imaging

MR imaging was performed by using a 1.5T system (Intera Achieva; Philips Medical Systems, Best, the Netherlands) before the initiation of treatment for both prospective and validation studies, with a maximum gradient strength of 66 mT/m, and a maximum slew rate of 160 mT/m/ms. MR imaging at an early phase of treatment also was performed for the prospective study. The FOV was 200–230 mm with a section thickness of 3–5 mm and a section gap of 0.5–1.5 mm, and a neurovascular coil with sensitivity encoding was used. The subjects were placed in a supine position. Pretreatment images were obtained at a median of 8 days before the start of radiation therapy for both prospective and validation studies. Early treatment-phase images were obtained a median of 7 days after the start of radiation therapy, with a median radiation dose of 10.8 Gy.

In the prospective study, T2-weighted turbo spin-echo, T1-weighted, diffusion-weighted, T2-calculated, and gadolinium-enhanced T1-weighted transverse images of the neck were obtained at pretreatment imaging, and coronal and/or sagittal images also were obtained when needed. For gadolinium-enhanced imaging, gadopentetate dimeglumine (Magnevist; Schering, Berlin, Germany), 0.1 mmol/kg body weight, was injected intravenously. In the validation study, the same MR imaging except T2-calculated imaging was obtained for all patients at pretreatment imaging. At early treatment-phase imaging, T2-weighted turbo spin-echo and/or T1-weighted, T2-calculated, and DWIs were obtained.

The imaging parameters for T2-weighted images were as follows: matrix of 512 × 288, turbo factor of 18, TR of 4467 ms, TE of 100 ms, NEX of 2, and examination duration of 2 minutes 27 seconds. The parameters for T1-weighted images were as follows: matrix of 512 × 288, TR of 572–618 ms, TE of 10 ms, NEX of 1, and examination duration of 2 minutes 17–47 seconds. Those for DWIs were as follows: matrix of 256 × 112; TR of 3000 ms; TE of 73 ms; b-factors of 0, 100, 200, 300, 500, 750, and 1000 s/mm²; δ of 26.08 ms; Δ of 35.96 ms;

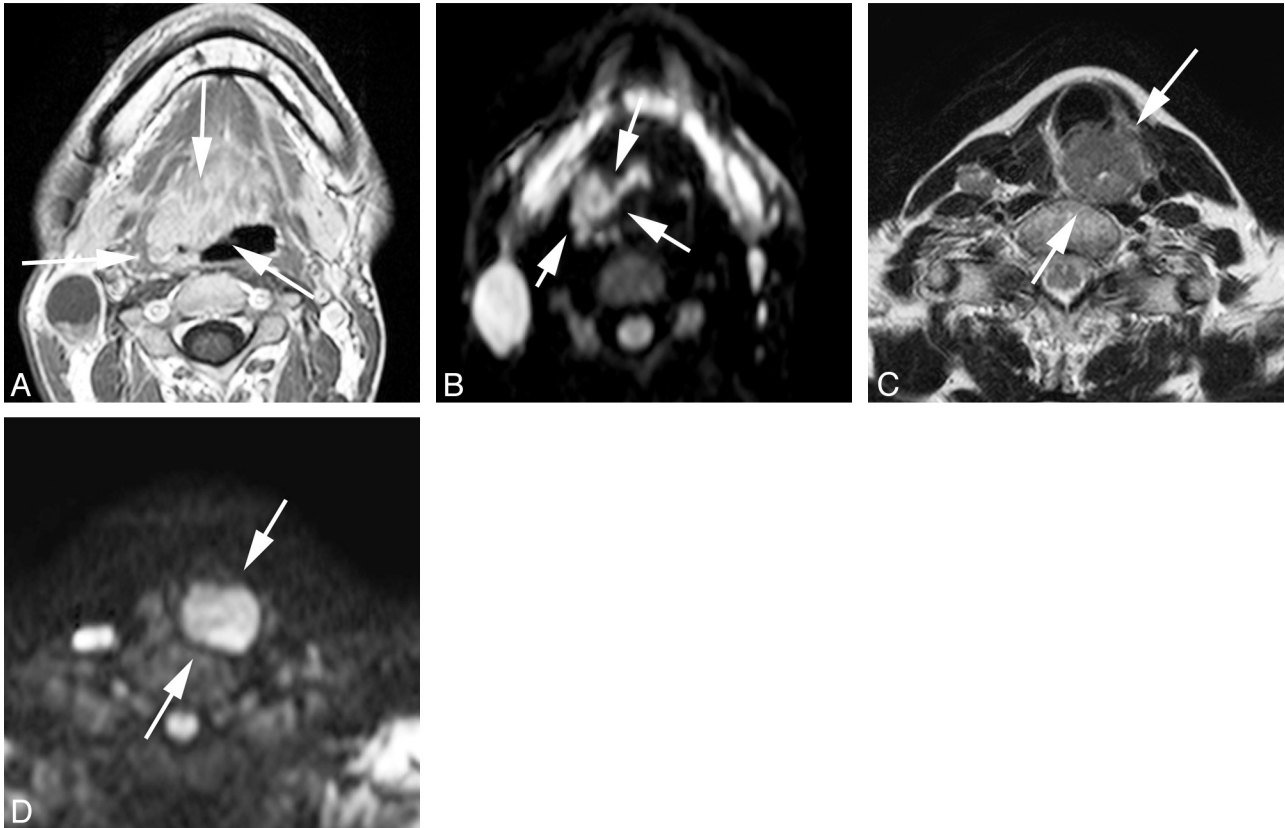


Fig 1. Representative images of local control and failure cases obtained before treatment. *A* and *B*, Transverse gadolinium-enhanced T1-weighted and DWI ($b = 1000 \text{ s/mm}^2$) of a local-control case (oropharyngeal cancer, 30s, male, T4N2M0, high ADC before treatment = $0.63 \times 10^{-3} \text{ mm}^2/\text{s}$). *C* and *D*, T2-weighted and DWI ($b = 1000 \text{ s/mm}^2$) of a local-failure case (hypopharyngeal cancer, 60s, female, T4N2M0, high ADC before treatment = $0.99 \times 10^{-3} \text{ mm}^2/\text{s}$). The arrows indicate primary lesions.

band width of 1645.9 Hz/pixel; NEX of 2; and examination duration of 4 minutes 6 seconds. DWI was obtained with a single-shot spin-echo echo-planar imaging sequence by using a spectral presaturation with inversion recovery for fat suppression. The motion-probing gradient pulses were placed along the x-, y-, and z-axes, and we used synthesized images from the 3 images. The imaging parameters for T2-calculated images were as follows: matrix of 256×256 ; TR of 3000 ms; TEs of 20, 40, 60, 80, 100, and 120 ms; NEX of 1; and examination duration of 8 minutes 12 seconds. Representative images are shown in Fig 1.

ADC Calculation

The ROI was designated as the primary lesion at the level of the largest tumor diameter on DWIs of each b-value to cover most of the lesion, while avoiding cystic or necrotic components with reference to T2-weighted, T1-weighted, and/or gadolinium-enhanced images. This procedure was done by consensus between M.H. and Y.M. without information regarding local failure or control (M.H. and Y.M. each have >15 years of experience in diagnostic radiology). The ADC was calculated as follows: The mean SIs of the ROI under various b-values were fitted to the equation $SI = SI_0 e^{-bD}$, where SI is the measured SI, SI_0 is SI at b-value of 0, b is the strength of the motion-probing gradient, and D is ADC. An ADC calculated with 4 different b-values of 0, 100, 200, and 300 s/mm^2 was taken as the value of low ADC and that with b-values of 300, 500, 750, and 1000 s/mm^2 as high ADC.

T2 Calculation

The ROI also was designated as the primary lesion at the level of the largest tumor diameter on T2-calculated images of each TE to cover

most of the lesion, while avoiding cystic or necrotic components. This procedure also was done by consensus between M.H. and Y.M. The SIs under various TEs were fitted to the equation $SI = SI_0 e^{-TE/T2}$, where SI is the measured SI and SI_0 is the SI at TE of 0.

Tumor Volume

The tumor volume was calculated by delineating the tumor contour on gadolinium-enhanced T1-weighted or T2-weighted spin-echo transverse images. This procedure also was carried out by consensus between M.H. and Y.M. without information regarding local failure or control.

Statistics

For the prospective study, the following variables were selected and tested for their correlation with local failure: age, tumor volume before treatment, tumor volume at the early phase of treatment, volume reduction ratio [$1 - (\text{tumor volume at the early phase of treatment}) / (\text{tumor volume before treatment})$], dose, overall treatment time, T2 before treatment, T2 at the early phase of treatment, T2 increase ratio [$(\text{T2 at the early phase of treatment}) / (\text{T2 before treatment}) - 1$], high ADC and low ADC before treatment, high ADC and low ADC at the early phase of treatment, high ADC and low ADC increase ratio [$(\text{high ADC at the early phase of treatment}) / (\text{high ADC before treatment}) - 1$], [low ADC at the early phase of treatment] / [low ADC before treatment] - 1, tumor location (hypopharynx versus other locations), treatment method (chemoradiotherapy versus radiation therapy alone), T stage (T 12 versus T 34), and N stage (N 01 versus N 23). We used *t* tests to compare age, tumor volume before treatment, tumor volume at the early phase of treatment, volume reduction ratio, dose, overall treatment time, T2 before treatment, T2 at the early

Table 1: Univariate and multivariate survival analyses of the prospective study (n = 17)

Variable	Univariate Analysis (Log Rank Test), <i>P</i>	Multivariate Analysis (Cox Proportional Hazard Test), <i>P</i>
Treatment method (chemoradiotherapy vs radiotherapy)	.0017	NS ^a
High ADC before treatment (≥ 0.86 vs < 0.86)	.0004	.0186
High ADC increase ratio (≥ 0.25 vs < 0.25)	.0022	NS

^a NS indicates $P \geq .05$.

phase of treatment, T2 increase ratio, low ADC before treatment, low ADC at the early phase of treatment, low ADC increase ratio, high ADC before treatment, high ADC at the early phase of treatment, and high ADC increase ratio between local control and failure. Fisher exact test was used to analyze the association between local failure and each of tumor location, treatment method, T stage, and N stage. In the univariate analysis, the curves for local control were estimated by using the Kaplan-Meier method, and the log rank test was used to test the difference between curves. The variables showing differences ($P < .05$) between local failure and control in the *t* test or those showing associations ($P < .05$) with local failure in Fisher exact probability test were analyzed. ROC curve analysis for differentiating local failure from local control was performed for high ADC before treatment and the high ADC increase ratio, which showed significant differences in the *t* test, to identify the optimal threshold for a binary classifier. With each threshold value of high ADC before treatment and the high ADC increase ratio obtained from ROC analysis, and with a treatment method that also showed significant association with local failure, a log rank test was performed. The variables showing association ($P < .05$) in the log rank test were further tested by multivariate analysis by using the Cox proportional hazard test for their association with local failure.

For the validation study, *t* test and Fisher exact probability test were used to test the clinical and imaging variables described above except those related to early-phase data (eg, high ADC at the early phase of treatment or high ADC increase ratio) or T2-related data because those were not obtained. A log rank test was performed for T treatment method; tumor volume before treatment; and high ADC before treatment, which showed significant association with local failure or significant differences in the *t* test; to test the correlation with local failure. The threshold values for tumor volume before treatment and high ADC before treatment were determined by using ROC analysis. The variables showing association ($P < .05$) in the log rank test were further tested by multivariate analysis by using the Cox proportional hazard test for their association with local failure. A 2×2 contingency table was produced, and Fisher exact probability test also was applied for tumor volume before treatment and high ADC before treatment. The correlation between tumor volume before treatment and high ADC before treatment was tested with a linear regression test.

Statistical calculations were performed by using statistical analysis software (JMP, version 7.0.1; SAS Institute, Cary, North Carolina; and Prism, version 5.02; GraphPad Software, San Diego, California). *P* values $< .05$ were considered statistically significant. Statistical analysis was carried out in consultation with a biostatistician at our institute.

Table 2: Univariate and multivariate survival analyses of the retrospective validation study (n = 40)

Variable	Univariate Analysis (Log Rank Test), <i>P</i>	Multivariate Analysis (Cox Proportional Hazard Test), <i>P</i>
T stage (T12 vs T34)	.0009	NS
Treatment method (chemoradiotherapy vs radiotherapy)	$< .0001$	NS
Tumor volume before treatment (≥ 9000 mm ³ vs < 9000)	.0002	.0217
High ADC before treatment (≥ 0.86 vs < 0.86)	$< .0001$.0001

^a NS indicates $P \geq .05$.

Results

In the prospective study, high ADC before treatment and the high ADC increase ratio revealed significant differences between local control and failure (On-line Table 1). The treatment method also showed a significant association with local failure (On-line Table 1). ROC analyses resulted in threshold values of 0.86×10^{-3} mm²/s for high ADC before treatment and 0.25 for the high ADC increase ratio. In univariate analysis by using the log rank test, high ADC before treatment ($\geq 0.86 \times 10^{-3}$ mm²/s versus < 0.86), the high ADC increase ratio (≥ 0.25 versus < 0.25), and the treatment method also showed significant correlation with local failure (Table 1). In multivariate analysis by using the Cox proportional hazard test, only high ADC before treatment revealed a significant correlation with local failure (Table 1).

In the validation study, tumor volume before treatment and high ADC before treatment showed significant differences between local control and failure (On-line Table 2). T stage and treatment method also showed significant correlation (On-line Table 2). ROC analysis resulted in a threshold value of 9000 mm³ for tumor volume before treatment. A threshold value for high ADC before treatment was also 0.86×10^{-3} mm²/s, as in the prospective study. In univariate analysis by using the log rank test, tumor volume before treatment (≥ 9000 mm³ versus < 9000), high ADC before treatment ($\geq 0.86 \times 10^{-3}$ mm²/s versus < 0.86), T stage, and treatment method also revealed a significant correlation with local failure (Table 2). In multivariate analysis by using the Cox proportional hazard test, tumor volume before treatment and high ADC before treatment showed significant association (Table 2). The local control curves regarding tumor volume before treatment and high ADC before treatment are shown in Fig 2. There was no significant correlation between tumor volume before treatment and high ADC before treatment (Fig 3). ROC analysis for tumor volume before treatment and high ADC before treatment resulted in AUCs of 0.749 and 0.977, respectively. A 2×2 contingency table based on a threshold tumor volume before treatment value showed a sensitivity of 0.846, specificity of 0.741, PPV of 0.611, NPV of 0.909, and accuracy of 0.775 ($P = .0007$, Fisher exact test; odds ratio = 15.7) and that based on a threshold high ADC before treatment value showed a sensitivity of 0.923, specificity of 0.963, PPV of 0.923, NPV of 0.963, and accuracy of 0.95 ($P < .0001$, Fisher exact test; odds ratio = 312).

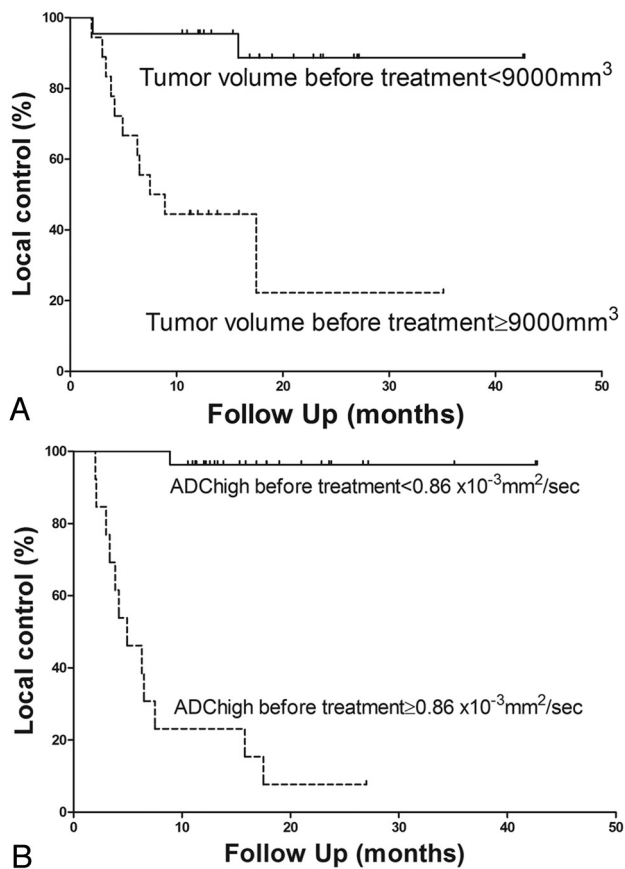


Fig 2. Comparison of local-control curves in the validation study. *A*, Comparison of the local-control curves between tumor volume before treatment $< 9000 \text{ mm}^3$ (solid line) and $\geq 9000 \text{ mm}^3$ (dashed line) ($P = .0002$). *B*, Comparison of the local-control curves between high ADC before treatment $< 0.86 \times 10^{-3} \text{ mm}^2/\text{sec}$ (solid line) and $\geq 0.86 \times 10^{-3} \text{ mm}^2/\text{sec}$ (dashed line) ($P < .0001$).

Discussion

Chemoradiotherapy has been increasingly chosen as a treatment option for advanced HNSCC because it preserves function and minimizes social losses. Therefore, it is of use to differentiate treatment-resistant cases from treatment-sensitive cases before or at the early phase of treatment. Then, more intensive treatment regimens or other treatment options such as surgery could be considered for the treatment-resistant cases. The results from the prospective study revealed that high ADC before treatment correlates with local failure of HNSCC treated with radiation therapy. According to the results from the prospective study, we considered that early phase MR imaging is not necessary for predicting local failure. Therefore, the inclusion criteria for the validation study were extended to those for whom early-phase MR imaging was not obtained. The results of the validation study indicated that high ADC before treatment along with tumor volume before treatment correlates with local failure in HNSCC treated with radiation therapy. We considered that high ADC before treatment would be a superior predictor for local failure based on the results from multivariate analysis and a 2×2 contingency table. The slight difference of the results between the prospective and validation studies was probably due to differences in the distributions of tumor volume and T stage. In the prospective study, patients with relatively small lesions were excluded because the lesion could not be detected clearly on an early-phase DWI, as described in the Patients section.

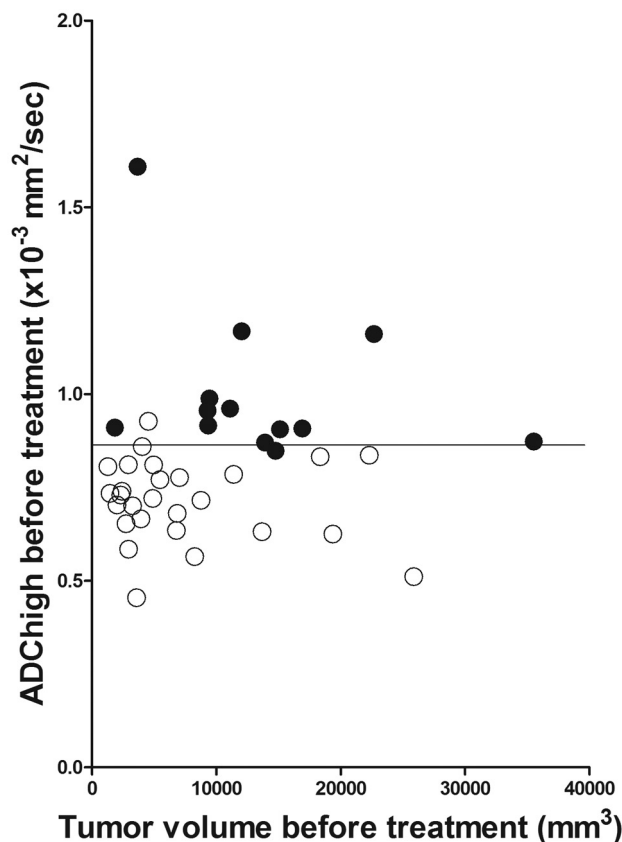


Fig 3. Scatterplot of tumor volume before treatment versus high ADC before treatment. Open and closed circles indicate local control and failure cases, respectively. Horizontal line indicates a threshold value of $0.86 \times 10^{-3} \text{ mm}^2/\text{s}$ for high ADC before treatment.

The result that the pretreatment ADC of the primary lesion in HNSCC correlates with local failure is in general consistent with the findings of previous reports, including ours. Kato et al¹⁹ reported that pretreatment ADC showed a weak inverse correlation with tumor regression rates in 28 cases. They evaluated the tumor regression rates based on either CT or MR imaging performed within 2 weeks after finishing chemotherapy and/or radiation therapy, with a median dose of 30 Gy (range, 20–40 Gy) according to the response evaluation criteria in solid tumors. We consider that local failure or control with > 6 months of follow-up duration would be more important for managing patients. In contrast, King et al²² reported that pretreatment ADC was not associated with local failure in a study analyzing 50 cases of HNSCC. We attribute these differences in results to the following. The studies used different methods for calculating ADC. King et al²² calculated ADC with b-values of 0, 100, 200, 300, 400, and 500 s/mm^2 . Low ADC calculated with b-values of 0, 100, 200, and 300 s/mm^2 also resulted in a lack of correlation with local failure in our study. We consider that ADC calculated with relatively high b-values would be appropriate for predicting treatment response because ADC calculated with relatively low b-values is strongly affected by perfusion.^{25,26}

The result that the ADC increase ratio at the early phase of treatment correlated with local failure is consistent with that of previous reports. Vandecaveye et al²¹ reported that ADC changes at 2 and 4 weeks after initiation of chemoradiotherapy or radiation therapy were correlated with locoregional failure

in a study with 30 HNSCCs, revealing that the cases with a high ADC increase ratio showed locoregional control. As for regional control, Kim et al²⁰ also reported that a low pretreatment ADC of nodes and a high increase ratio of the ADC of nodes at 1 week after treatment initiation predicted regional control in a study with 33 HNSCCs. Finally, in an experimental study by using a mouse model of squamous cell carcinoma, Hamstra et al²⁷ reported that a group treated with chemoradiotherapy showed better prognoses, and demonstrated a significant increase in ADC.

In the present study, tumor volume change at the early phase of treatment did not correlate with local failure. Vandecaveye et al²¹ reported that the prediction of locoregional failure by using volume change at 2 or 4 weeks after initiation of treatment was inferior to that by using ADC change. The timing of MR imaging in the present study, a median of 7 days after the initiation of treatment and a median of 10.8 Gy, might have been too early to detect a correlation.

As for the accuracy of the clinical outcome prediction, Vandecaveye et al²¹ reported that the prediction of locoregional control by using ADC change at 2 weeks after initiation of chemoradiotherapy resulted in an AUC of 0.94, with 88% sensitivity, 91% specificity, 78% PPV, 96% NPV, and 90% accuracy and that using ADC change at 4 weeks resulted in an AUC of 0.97, with 100% sensitivity, 91% specificity, 80% PPV, 100% NPV, and 94% accuracy in a study with 33 cases. King et al²² reported that the prediction of locoregional control by using the ADC change pattern resulted in 80% sensitivity, 100% specificity, 100% PPV, 83% NPV, and 90% accuracy in a study with 20 cases showing residual masses. As described in the Results section, our present findings in a retrospective validation study with 40 cases were comparable to theirs (AUC of 0.977, 92.3% sensitivity, 96.3% specificity, 92.3% PPV, 96.3% NPV, and 95% accuracy). The advantages of using pretreatment ADC to predict treatment response are as follows: 1) the prediction would be completed before the initiation of treatment, 2) additional MR examinations would not be necessary, and 3) patients with relatively small primary lesions would not be excluded.

There have been studies investigating the relation between MR imaging findings other than the ADC and treatment response in HNSCC.^{28,29} Enhanced MR imaging requires contrast material that may elicit side effects, require additional expense, and be inapplicable to patients with severe renal dysfunction. We therefore consider that the prediction of local failure by using pretreatment ADC would be superior.

A limitation of this study is that the total number of patients analyzed was small. A prospective study with a larger number of patients may be needed to confirm the results.

Conclusions

Our study suggests that ADC calculated with relatively high b-values (300, 500, 750, and 1000 s/mm²) before treatment, as well as tumor volume before treatment, correlate with local failure of primary HNSCC treated with radiation therapy. More intensive treatment regimens such as dose escalation or other treatment options such as surgical resection may be con-

sidered for the patients showing high ADC value before treatment.

Acknowledgment

We thank Junji Kishimoto, PhD (Department of Digital Medicine Initiative, Kyushu University) for statistical consultations.

References

1. Tanner JE. Self diffusion of water in frog muscle. *Biophys J* 1979;28:107–16
2. Tanner JE. Intracellular diffusion of water. *Arch Biochem Biophys* 1983;224:416–28
3. Hatakenaka M, Matsuo Y, Setoguchi T, et al. Alteration of proton diffusivity associated with passive muscle extension and contraction. *J Magn Reson Imaging* 2008;27:932–37
4. Hatakenaka M, Yabuuchi H, Sunami S, et al. Joint position affects muscle proton diffusion: evaluation with a 3-T MR system. *AJR Am J Roentgenol* 2010;194:W208–11
5. Wang J, Takashima S, Takayama F, et al. Head and neck lesions: characterization with diffusion-weighted echo-planar MR imaging. *Radiology* 2001;220:621–30
6. Guo Y, Cai YQ, Cai ZL, et al. Differentiation of clinically benign and malignant breast lesions using diffusion-weighted imaging. *J Magn Reson Imaging* 2002;16:172–78
7. Eida S, Sumi M, Sakihama N, et al. Apparent diffusion coefficient mapping of salivary gland tumors: prediction of the benignancy and malignancy. *AJNR Am J Neuroradiol* 2007;28:116–21
8. Sumi M, Ichikawa Y, Nakamura T. Diagnostic ability of apparent diffusion coefficients for lymphomas and carcinomas in the pharynx. *Eur Radiol* 2007;17:2631–37
9. Hatakenaka M, Soeda H, Yabuuchi H, et al. Apparent diffusion coefficients of breast tumors: clinical application. *Magn Reson Med Sci* 2008;7:23–29
10. Mardor Y, Roth Y, Ochershvilli A, et al. Pretreatment prediction of brain tumors' response to radiation therapy using high b-value diffusion-weighted MRI. *Neoplasia* 2004;6:136–42
11. Oh J, Henry RG, Pirzkal A, et al. Survival analysis in patients with glioblastoma multiforme: predictive value of choline-to-N-acetylaspartate index, apparent diffusion coefficient, and relative cerebral blood volume. *J Magn Reson Imaging* 2004;19:546–54
12. Higano S, Yun X, Kumabe T, et al. Malignant astrocytic tumors: clinical importance of apparent diffusion coefficient in prediction of grade and prognosis. *Radiology* 2006;241:839–46
13. Murakami R, Sugahara T, Nakamura H, et al. Malignant supratentorial astrocytoma treated with postoperative radiation therapy: prognostic value of pretreatment quantitative diffusion-weighted MR imaging. *Radiology* 2007;243:493–99
14. Chenevert TL, Stegman LD, Taylor JM, et al. Diffusion magnetic resonance imaging: an early surrogate marker of therapeutic efficacy in brain tumors. *J Natl Cancer Inst* 2000;92:2029–36
15. Mardor Y, Pfeffer R, Spiegelmann R, et al. Early detection of response to radiation therapy in patients with brain malignancies using conventional and high b-value diffusion-weighted magnetic resonance imaging. *J Clin Oncol* 2003;21:1094–100
16. Hamstra DA, Chenevert TL, Moffat BA, et al. Evaluation of the functional diffusion map as an early biomarker of time-to-progression and overall survival in high-grade glioma. *Proc Natl Acad Sci U S A* 2005;102:16759–64
17. Moffat BA, Chenevert TL, Lawrence TS, et al. Functional diffusion map: a noninvasive MRI biomarker for early stratification of clinical brain tumor response. *Proc Natl Acad Sci U S A* 2005;102:5524–29
18. Koh DM, Scurr E, Collins D, et al. Predicting response of colorectal hepatic metastasis: value of pretreatment apparent diffusion coefficients. *AJR Am J Roentgenol* 2007;188:1001–08
19. Kato H, Kanematsu M, Tanaka O, et al. Head and neck squamous cell carcinoma: usefulness of diffusion-weighted MR imaging in the prediction of a neoadjuvant therapeutic effect. *Eur Radiol* 2009;19:103–09
20. Kim S, Loevner L, Quon H, et al. Diffusion-weighted magnetic resonance imaging for predicting and detecting early response to chemoradiation therapy of squamous cell carcinomas of the head and neck. *Clin Cancer Res* 2009;15:986–94
21. Vandecaveye V, Dirix P, De Keyser F, et al. Predictive value of diffusion-weighted magnetic resonance imaging during chemoradiotherapy for head and neck squamous cell carcinoma. *Eur Radiol* 2010;20:1703–14
22. King AD, Mo FK, Yu KH, et al. Squamous cell carcinoma of the head and neck: diffusion-weighted MR imaging for prediction and monitoring of treatment response. *Eur Radiol* 2010;20:2213–20
23. Hatakenaka M, Nakamura K, Yabuuchi H, et al. Pretreatment apparent diffu-

- sion coefficient of the primary lesion correlates with local failure in head-and-neck cancer treated with chemoradiotherapy or radiotherapy. *Int J Radiation Oncology Biol Phys* 2011;81:339–45
24. O'Sullivan B. **Nasopharynx cancer: therapeutic value of chemoradiotherapy.** *Int J Radiat Oncol Biol Phys* 2007;69:S118–21
25. Le Bihan D, Breton E, Lallemand D, et al. **Separation of diffusion and perfusion in intravoxel incoherent motion MR imaging.** *Radiology* 1988;168:497–505
26. Yamada I, Aung W, Himeno Y, et al. **Diffusion coefficients in abdominal organs and hepatic lesions: evaluation with intravoxel incoherent motion echo-planar MR imaging.** *Radiology* 1999;210:617–23
27. Hamstra DA, Lee KC, Moffat BA, et al. **Diffusion magnetic resonance imaging: an imaging treatment response biomarker to chemoradiotherapy in a mouse model of squamous cell cancer of the head and neck.** *Transl Oncol* 2008;1:187–94
28. Ljumanovic R, Langendijk JA, van Waddingen M, et al. **MR imaging predictors of local control of glottic squamous cell carcinoma treated with radiation alone.** *Radiology* 2007;244:205–12
29. Cao Y, Popovtzer A, Li D, et al. **Early prediction of outcome in advanced head-and-neck cancer based on tumor blood volume alterations during therapy: a prospective study.** *Int J Radiat Oncol Biol Phys* 2008;72:1287–90